

Separation induced resonances in quasi-one-dimensional ultracold atomic gases

Wenbo Fu,¹ Zhenhua Yu,² and Xiaoling Cui^{1*}

¹*Institute for Advanced Study, Tsinghua University, Beijing, 100084*

²*Department of Physics, Ohio State University, Columbus, OH 43210*

(Dated: October 27, 2018)

We study the effective one-dimensional (1D) scattering of two distinguishable atoms confined individually by *separated* transverse harmonic traps. With equal trapping frequency for two s-wave interacting atoms, we find that by tuning the trap separations, the system can undergo *double* 1D scattering resonance, named as the separation induced resonance(SIR), when the ratio between the confinement length and s-wave scattering length is within (0.791, 1.46]. Near SIR, the scattering property shows unique dependence on the resonance position. The universality of a many-body system on scattering branch near SIR is demonstrated by studying the interaction effect of a localized impurity coupled with a Fermi sea of light atoms in a quasi-1D trap.

I. INTRODUCTION

Ultracold atomic gases have provided unprecedented accesses to fascinating strongly interacting many-body systems, especially those in unitary limit with resonant scattering. Besides Feshbach resonances, various external confinements are recognized as another efficient way to achieve resonances in all dimensions[1–5], and there have been successful explorations of resonance scattering properties in experiments[6–10].

The mechanism of confinement induced resonance was first explored by Bergeman *et al.*[2]. A bound state constructed in the Hilbert space spanned by the excited transverse states of non-interacting Hamiltonian was introduced as a closed channel bound state(CCBS). By tuning the confinements the resonance occurs when CCBS touches the scattering threshold. This class of resonance can also be understood as the consequence of modified low-energy scattering theory by properly renormalizing all virtual scatterings to high-energy states[11]. The properties of these resonances closely depend on the type of confinement potentials. Previous studies have shown that within the contact interaction model, all the induced resonances fall into two classes. If the trapping potential decouples relative motion(r) from center-of-mass(R), the only one CCBS would induce a *single* resonance such as in Ref.[1–3]; if not, there would be an infinite number of CCBS due to the coupling between r and all R -channels, resulting in an infinite number of resonances such as in Ref.[4, 5]. Therefore an interesting question is whether these two classes have covered all the possible resonances under external confinements. In this paper, by providing an alternative class of scattering resonance induced by trap separations(see below), we show the answer is *no*.

We consider two distinguishable atoms confined individually by transverse harmonic traps with tunable separations (see Fig.1(a)). We find two resonances of one-dimensional(1D) scattering by tuning the separation,

which we name as “separation induced resonance” (SIR). It is the non-monotonic evolution of CCBS with the separation that gives rise to the emergence of two resonances, and also leads to new features in parameters describing the effective 1D scattering. By introducing such a system, we show an interesting class of induced resonances as SIR. For such resonances, the number of resonances is not solely determined by the number of CCBS, and the effective 1D scattering strength exhibits exotic dependence on the tunable parameter as shown by Fig.3. All these features are qualitatively different from those of Feshbach resonances and previously studied confinement induced resonances. Our finding substantially enriches the existing understanding of the induced resonance physics. In addition, we study the many-body physics across SIR. By employing an impurity problem, we show that a many-body system on metastable scattering branch can go across double SIRs and exhibit universal properties at each resonance. The two-body bound state is also studied, and experimental realizations and detections are discussed finally.

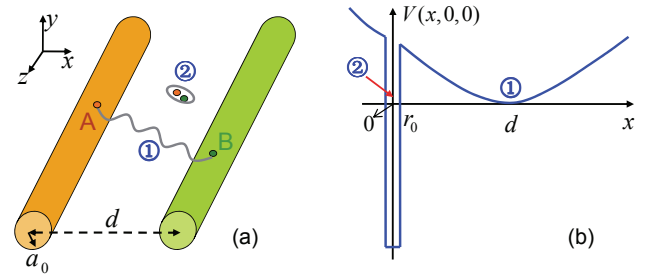


FIG. 1: (Color online) Schematic plot of system setup. (a) Two interacting atoms(A, B) are separately confined in transverse harmonic traps with characteristic length a_0 and distance d . (b) Potentials $V(x, 0, 0)$ in the center-of-mass frame, including trapping potential centered at $\mathbf{r} = (d, 0, 0)$ (①) and short-range($r_0 \simeq 0$) interaction at $\mathbf{r} = 0$ (②).

The rest of the paper is organized as follows. In section II, we present the formulism for effective 1D scattering across SIR. In section III we discuss the origin of double resonances and show the unique features of

*Electronic address: xlcui@mail.tsinghua.edu.cn

effective scattering strength near resonances. The two-body bound state is studied in Section IV. Section V is contributed to the impurity problem, from which we address the universal property of a many-body system at metastable scattering branch across SIR. We discuss the experimental realization and finally remark on the generalization of SIR to other systems in Section VI.

II. EFFECTIVE SCATTERING IN 1D

We consider two distinguishable atoms, A and B, respectively trapped by transverse potentials $V_t(\mathbf{r}_A) = m_A \omega^2 ((x_A + d/2)^2 + y_A^2)/2$ and $V_t(\mathbf{r}_B) = m_B \omega^2 ((x_B - d/2)^2 + y_B^2)/2$, which decouples the center-of-mass and relative motions. The Hamiltonian for the relative motion is $H_{rel}(\mathbf{r}) = H_0 + U(\mathbf{r})$, where (we take $\hbar = 1$ throughout the paper)

$$H_0 = -\frac{\nabla_{\mathbf{r}}^2}{2\mu} + \frac{\mu}{2}\omega^2((x-d)^2 + y^2), \quad (1)$$

$U(\mathbf{r}) = \frac{2\pi a_s}{\mu} \delta(\mathbf{r}) \frac{\partial}{\partial r} r|_{r \rightarrow 0}$, with the reduced mass $\mu = m_A m_B / (m_A + m_B)$ and the s-wave scattering length a_s . H_0 determines the spectrum as $E = E_{n_x, n_y} + k^2/(2\mu)$, with $E_{n_x, n_y} = (n_x + n_y + 1)\omega$ the eigen-energies for the transverse eigen-states $\phi_{n_x, n_y}(x, y) \equiv \psi_{n_x}(x-d)\psi_{n_y}(y)$, $n_x, n_y = 0, 1, 2, \dots$ (ψ_n is the 1D harmonic oscillator wavefunctions).

In this system, the low energy scattering processes for incoming wave functions with $n_x = n_y = 0$ and $k^2/2\mu \ll \omega$ can be described by a 1D Hamiltonian for the relative motion (along z-direction) as $h_{rel} = -(1/2\mu)(d^2/dz^2) + g_{1D}\delta(z)$, with g_{1D} the 1D coupling strength[1]. To derive g_{1D} in terms of a_s , we study the scattering wave function at low energy $E = \omega + k^2/(2\mu)$,

$$\Psi(\mathbf{r}) = \phi_{0,0}(x, y)e^{ikz} + fG(\mathbf{r}, 0), \quad (2)$$

where the Green function, $G(\mathbf{r}, 0) = \langle \mathbf{r} | \frac{1}{E - H_0 + i\delta} | 0 \rangle$, is expressed as

$$G(\mathbf{r}, 0) = \sum_{n_x, n_y} \int_{-\infty}^{\infty} \frac{dp}{2\pi} \frac{\phi_{n_x, n_y}(x, y)e^{ipz} \phi_{n_x, n_y}^*(0, 0)}{E - E_{n_x, n_y} - p^2/(2\mu) + i\delta}. \quad (3)$$

To solve the problem, it is essential to write the asymptotic form of Eq.3 at $\mathbf{r} \rightarrow 0$ as $G(r, 0) = -\frac{\mu}{2\pi r} + C(ka_0, \tilde{d}) + o(r)$, where $a_0 = \sqrt{1/\mu\omega}$ is the characteristic length of the harmonic oscillator, $\tilde{d} = d/a_0$. With the help of the imaginary-time evolution operator of harmonic oscillator[4], we obtain $C = \frac{\partial}{\partial r}(rG(r, 0))_{r \rightarrow 0}$ as

$$C(ka_0, \tilde{d}) = \frac{\mu}{\pi a_0} \left[\frac{1}{ika_0} e^{-\tilde{d}^2} - \frac{1}{\sqrt{2\pi}} A(ka_0, \tilde{d}) \right], \quad (4)$$

and

$$A(ka_0, \tilde{d}) = \int_0^{\infty} \frac{d\tau}{\sqrt{\tau}} e^{\frac{k^2 a_0^2 \tau}{2}} \left(\frac{e^{-\tilde{d}^2 \tanh \frac{\tau}{2}}}{1 - e^{-2\tau}} - \frac{e^{-\frac{k^2 a_0^2 \tau}{2}}}{2\tau} - e^{-\tilde{d}^2} \right). \quad (5)$$

According to the Schrodinger equation $H_{rel}\Psi = E\Psi$, we find the scattering amplitude as

$$f = \phi_{0,0}(0, 0) \left[\frac{\mu}{2\pi a_s} - C(ka_0, \tilde{d}) \right]^{-1}, \quad (6)$$

thus we obtain the closed form of Eq.2. When $d = 0$, all equations reproduce the well-known quasi-1D results[1, 2]. More detailed derivation of Eq.4 is given in Appendix A.

At large distances along z-direction, all terms in the Green function (Eq.3) decays except for the lowest transverse mode with $n_x = n_y = 0$ [1]. Since $U(\mathbf{r})$ only takes effect at $r = 0$ but vanishes otherwise, the part of $\Psi(\mathbf{r})$ with even-parity of z , $\Psi_{\text{even}}(\mathbf{r}) = \frac{1}{2}(\Psi(x, y, z) + \Psi(x, y, -z))$, is scattered while the odd-parity part remains unaltered. By Eq. (2), $\Psi_{\text{even}}(\mathbf{r}) = \phi_{0,0}(x, y)e^{i\delta_k} \cos(k|z| + \delta_k)$, where the phase shift δ_k satisfies

$$\tan \delta_k = -\frac{2}{ka_0} e^{-\tilde{d}^2} \left[\frac{a_0}{a_s} + \sqrt{\frac{2}{\pi}} A(ka_0, \tilde{d}) \right]^{-1}. \quad (7)$$

In the effective 1D limit ($ka_0 \ll 1$), we find $A(ka_0, \tilde{d}) = A(0, \tilde{d}) + \lambda_d (ka_0)^2 + o(k^4 a_0^4)$, where $0 < \lambda_d \leq 0.666$ for all \tilde{d} as shown by Fig.6 in Appendix B. [See more details regarding the property of $A(ka_0, \tilde{d})$ in Appendix B]. Therefore for low-energy scattering, we neglect the energy-dependence in A-function and approximate the coupling strength at different $k \ll 1/a_0$ to be a constant given by $g_{1D} = -\lim_{k \rightarrow 0} k \tan \delta_k / \mu$. To this end, we obtain the relation between g_{1D} and a_s .

According to Eq.7, the separation induced resonance (SIR) for $k \rightarrow 0$ occurs at

$$\frac{a_0}{a_s} = -\sqrt{\frac{2}{\pi}} A(0, \tilde{d}), \quad (8)$$

when $g_{1D} = \infty$, $|\delta| = \pi/2$. In Fig.2(a) we plot the right-hand-side of Eq.8, which is the required value of a_0/a_s for 1D scattering resonance at given \tilde{d} . According to the properties of $A(0, \tilde{d})$ as given by Eqs.(B4,B5) in Appendix B, we obtain the asymptotic expression of a_0/a_s at SIR for small \tilde{d} as $[a_0/a_s]_{\text{SIR}} \approx 1.46 - 1.39\tilde{d}^2$, and for large \tilde{d} as $[a_0/a_s]_{\text{SIR}} \approx \tilde{d} - 1/\tilde{d}$. In the limit of large \tilde{d} and also large a_0/a_s , the mechanism for SIR can be understood in the following intuitive way. When a tightly bound molecule (play the role as CCBS[2]) is formed, the relative wave function of the molecule concentrate around $r = 0$ (shown as ② in Fig.1). Its energy is approximately the sum of internal binding energy due to interaction, $-1/2\mu a_s^2$, and external potential energy due to trap separations, $\mu\omega^2 d^2/2$; the resonance occurs when the total energy matches the threshold of free particles (shown as ① in Fig.1), i.e., $-1/2\mu a_s^2 + \mu\omega^2 d^2/2 = \omega$, which is exactly the criterion as extracted from Eq.(8) and Eq.(B5). For intermediate \tilde{d} , there is a minimum of $[a_0/a_s]_{\text{SIR}}$ as 0.791 found at $\tilde{d} = 1.123$. Remarkably, for fixed $a_0/a_s \in (0.791, 1.46]$, the system undergoes two distinctive resonances as \tilde{d} increases from zero.

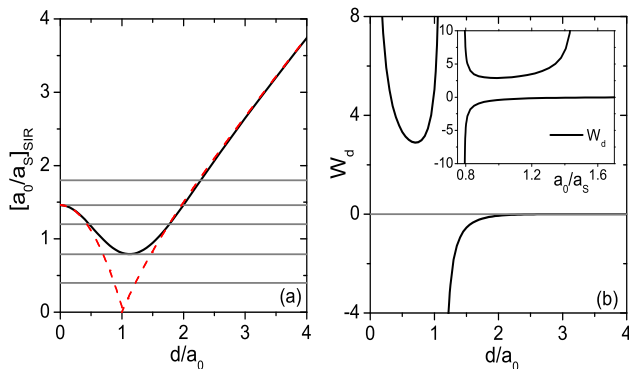


FIG. 2: Separation induced resonance(SIR) in quasi-1D system. (a) a_0/a_s as a function of $\tilde{d} = d/a_0$ at SIR. Dashed lines are the functional fit to $1.46 - 1.39\tilde{d}^2$ in small \tilde{d} , and $\tilde{d} - 1/\tilde{d}$ in large \tilde{d} limit. The horizontal lines label five coupling strengths (from bottom to top): $a_0/a_s = 0.4, 0.791, 1.2, 1.46, 1.8$, with further properties shown in Fig.3,4. (b) Resonance width W_d versus resonance position \tilde{d} and corresponding a_0/a_s (inset).

III. BASIC FEATURES OF SIR

In this section we address the basic features of SIR. First we explore the origin of double resonances, and secondly we study the resulted structure of effective scattering strength across SIR and corresponding resonance width.

A. Origin of double resonances

The origin of double resonances can be understood by studying the CCBS that is constructed by all excited transverse modes of H_0 . The binding energy of the CCBS, $E_b^c = E - \omega$, is given by

$$\frac{\mu}{2\pi a_s} = \lim_{r \rightarrow 0} (G^c(r, 0) + \frac{\mu}{2\pi r}), \quad (9)$$

where G^c is the closed channel Green function which follows Eq.3 but excludes $n_x = n_y = 0$ in the summation. Thus Eq.9 is equivalent to

$$\frac{a_0}{a_s} = -\sqrt{\frac{2}{\pi}} A\left(\sqrt{\frac{2E_b^c}{\omega}}, \tilde{d}\right), \quad (10)$$

Compared with Eq. (8), we see that SIR occurs when $E_b^c = 0$, i.e., when the CCBS touches the threshold.

The intriguing dependence of the resonance position on \tilde{d} is a direct consequence of that of E_b^c on \tilde{d} . In Fig.3(a), we show that for given a_0/a_s , E_b^c decreases with \tilde{d} at small \tilde{d} but increases at large \tilde{d} . Mathematically this is attributed to the non-monotonic behavior of A -function(Eq.(5)) when increasing \tilde{d} . For fixed E_b^c , A -function increases/decreases with \tilde{d} in the small/large \tilde{d} limit (particularly these properties are

shown in Eqs.(B4,B5) for $A(0, \tilde{d})$); while for fixed \tilde{d} , A -function always increases with the energy. These properties together give rise to the non-trivial dependence of E_b^c on \tilde{d} as solved from Eq.(10) for each given a_0/a_s . Physically, the non-trivial behavior of E_b^c can be explained in the following way. The explicit form of G^c in Eq. (9) (cf. Eq. (3)) indicates that d affects E_b^c only through the coupling weight $\alpha_{n_x, n_y} = |\phi_{n_x, n_y}(0, 0)|^2 = \psi_{n_x}^2(-d)\psi_{n_y}^2(0)$, particularly the $\psi_{n_x}^2(-d)$ part. Unlike $d = 0$ case where the interaction only couples even-parity states ($n_x = 0, 2, \dots$), non-zero d additionally mix all odd-parity states ($n_x = 1, 3, \dots$) into $\Psi(\mathbf{r})$. When $\tilde{d} \ll 1$, α_{n_x, n_y} increases with \tilde{d} for all odd n_x , while decreases for all even n_x . We find that the former effect dominates so that small nonzero \tilde{d} facilitates the formation of CCBS and gives lower $E_b^c(d) \approx E_b^c(0) - 3d^2/(2\mu a_0^4)$. When $\tilde{d} \gg 1$, the coupling for both even and odd n_x decays exponentially with \tilde{d} . E_b^c in this limit approaches ω from below, implying two uncorrelated atoms when trapped far apart.

As analyzed above, for any given a_0/a_s , E_b^c as a function of \tilde{d} first decreases and then increases. As shown in Fig. 3, for small $a_0/a_s < 0.791$ the interaction is not strong enough to make E_b^c even touch the threshold and there is no resonance; for large $a_0/a_s > 1.46$, the interaction is so strong that at $d = 0$ the CCBS is already below the threshold, and therefore the resonance is only possible at large \tilde{d} ; however, for intermediate $a_0/a_s \in (0.791, 1.46]$, E_b^c is able to cross zero twice due to its non-monotonic behavior, and correspondingly g_{1D} diverges whenever E_b^c across zero. This is the origin of double resonance feature.

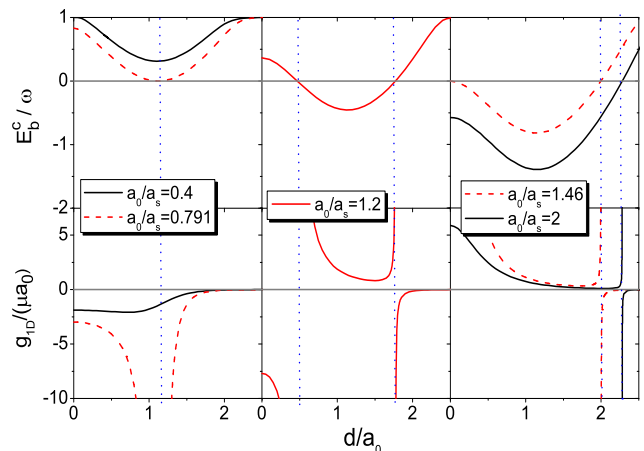


FIG. 3: The binding energy of CCBS (E_b^c/ω) and the effective 1D coupling strength ($g_{1D}/(\mu a_0)$) as functions of d/a_0 , for several typical values of a_0/a_s that correspond to five horizontal lines in Fig.2a. Vertical blue lines denote the resonance positions \tilde{d}_{res} , where $E_b^c = 0$ and $g_{1D} = \infty$.

B. g_{1D} near SIR

Near SIR, g_{1D} can be parameterized as $\tilde{g}_{1D}[\equiv g_{1D}\mu a_0] = W_d/(\tilde{d} - \tilde{d}_{res})$, with

$$W_d = \sqrt{2\pi}e^{-\tilde{d}^2} \left[\frac{\partial A(0, \tilde{d})}{\partial \tilde{d}} \right]_{res}^{-1}. \quad (11)$$

Here W_d is the width of SIR, analogous to that defined in Feshbach resonance[12]. In our system, W_d reflects the coupling strength between the open and closed channel responsible for SIR, and also determines how well SIR can be accessed in experiment due to the limited resolution of trap separations.

An important feature of SIR is that *the resonance width strongly depends on the resonance position, which changes sign at $\tilde{d}_{res} = 1.123$* . We show in Fig.2(b) how W_d changes with \tilde{d}_{res} and corresponding a_0/a_s . Due to the vanishing $\frac{\partial A(0, \tilde{d})}{\partial \tilde{d}}$ around $\tilde{d}_{res} = 0$ and 1.123 , W_d also experiences divergent behavior asymptotically as $W_d \sim 1/\tilde{d}_{res}$ and $W_d \sim -1/(\tilde{d}_{res} - 1.123)$ respectively. At the left(right) side of $\tilde{d}_{res} = 1.123$, W_d is positive(negative). Particularly, for a given $a_0/a_s \in (0.791, 1.46]$ the system accomplishes two SIRs: one of them is with large positive W_d and the other with small negative W_d (see the inset of Fig.2(b)); the opposite signs of these two W_d determine that g_{1D} keeps sign between two SIRs (see Fig.3), in contrast with Feshbach resonance where a_s crosses zero between two adjacent resonances.

In the limit of $a_0/a_s, \tilde{d}_{res} \gg 1$, W_d exponentially decays as $W_d = -2e^{-\tilde{d}^2}$. Physically such a narrow width corresponds to the very weak overlap of the wavefunctions of interacting particles, i.e., A and B atoms have little probability to collide with each other when they are trapped far apart. Note that the width defined in Eq.11 is meaningful for the realistic detection of SIR in experiment, but should not be confused with the narrow width effect in a magnetic Feshbach resonances[13]. In fact, as shown in Appendix B, the k-dependence of g_{1D} is always very weak and even negligible in $\tilde{d} \gg 1$ limit although the resonance width is exponentially small.

IV. TWO-BODY BOUND STATE

The true two-body bound state is given by the pole of the scattering amplitude, $f(i\kappa) = \infty$, i.e.,

$$\frac{\mu}{2\pi a_s} = C(i\kappa a_0, \tilde{d}). \quad (12)$$

In Fig.4(a) the binding energy, $E_b = E - \omega = -\kappa^2/(2\mu)$, is plotted as a function of \tilde{d} . We see that E_b always exists below zero for any a_s and d , due to the inclusion of $n_x = n_y = 0$ mode and the effective 1D density of state at low energies. Moreover, E_b monotonically decreases with \tilde{d} , which is dramatically different from E_b^c . In weak coupling limit ($a_s/a_0 \rightarrow 0^-$), the

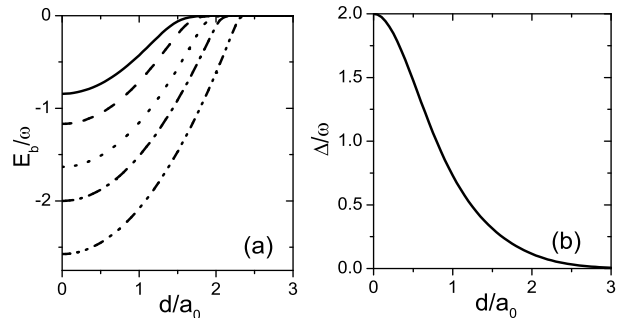


FIG. 4: (a) Binding energy of two-body bound state E_b as a function of d/a_0 for different $a_0/a_s = 0.4, 0.791, 1.2, 1.46, 1.8$ (from top to bottom). (b) Energy difference between CCBS and two-body bound state, $\Delta = E_b^c - E_b$, right at SIR as a function of resonance position d/a_0 .

bound state is merely the 1D consequence which gives $E_b = -\frac{\mu g_{1D}^2}{2} = -\frac{2a_s^2}{\mu a_0^4} e^{-2\tilde{d}^2}$. In the strong coupling limit ($a_s/a_0 \rightarrow 0^+$), for small \tilde{d} it is straightforward to obtain the binding energy as $E_b(\tilde{d}) = E_b(0) + \mu\omega^2 \tilde{d}^2/2$, which is shifted up exactly by the potential barrier; for large \tilde{d} , E_b would be very small and exponentially decay as $E_b = -2[\mu a_0^2(\tilde{d} - a_0/a_s)^2]^{-1} e^{-2\tilde{d}^2}$. To explore the difference between the CCBS and true two-body bound state, we plot in Fig.4(b) their energy difference, $\Delta = E_b^c - E_b$, right at SIR as a function of \tilde{d} . When $d = 0$, $\Delta = 2\omega$ reproduces the result in Ref.[1]. As \tilde{d} increases, Δ decreases and becomes exponentially small in the large \tilde{d} limit.

V. UNIVERSALITY OF SCATTERING BRANCH AT SIR

The universal property of a many-body system at SIR can be effectively explored by considering the following exactly solvable impurity problem. Consider that atoms A ($m_A = m$) form a Fermi-sea with Fermi energy k_F and interact with a localized impurity B ($m_B = \infty$) at the origin. In this case the Hamiltonian for A is exactly H_{rel} with $\mu = m$ (cf. Fig.1(b)). The same phenomenon of double SIRs can be deduced for A moving in the effective 1D tube.

Suppose the tube is with boundary $[-L, L]$, the allowed wave vectors are given by $kL + \delta_k = (n + \frac{1}{2})\pi$ ($n = 0, 1, \dots$). Given that there is no occupation of possible bound states, the non-zero phase shifts δ_k give rise to the interaction energy (or the energy difference from non-interacting case) as[14]

$$E_{int} = -\frac{1}{m\pi} \int_0^{k_F} k \delta_k dk. \quad (13)$$

Note that the scattering states contributing to E_{int} here

belong to the metastable scattering branch in quasi-1D in which $-\pi < \delta_k < 0$ for all k . Explicitly, the metastable branch corresponds to a Hilbert space expanded by scattering states, i.e., without the occupation of molecules. One typical example is the repulsive Fermi gas in 3D with positive a_s , and recently there have been extensive studies of single impurity problem in such system both theoretically[15] and experimentally[16]. Moreover, the scattering branch has also been realized in the bosonic quasi-1D system[7] in the absence of trap separations. In our system with trap separations, as shown in Fig.4, a two-body bound state always exists below the threshold for any a_s and \tilde{d} , whose binding energy monotonically decreases as \tilde{d} increases. This indicates that in a many-body system the universality is only possible for the metastable scattering branch which excludes the Hilbert space of molecules.

According to Eq.7, in Fig.5(a) we plot δ_k as a function of \tilde{d} for different momenta k . Considering $ka_0 \ll 1$, we have used k -independent $A(0, \tilde{d})$ in Eq.7, which will bring a negligible correction of the order of $o((ka_0)^2)$. We see that all the curves with different k cross exactly at the location of SIR. This is due to the *universal* phase shift as $-\pi/2$ right at SIR for all values of k , and according to Eq.13 this further leads to the *universal* interaction energy as half of the Fermi energy, $E_{int} = E_F/2$, at any position of SIR (see Fig.5(b)). According to Eq.7 and Eq.11, the slopes of δ and E_{int} across SIR are both inversely proportional to the resonance width W_d .

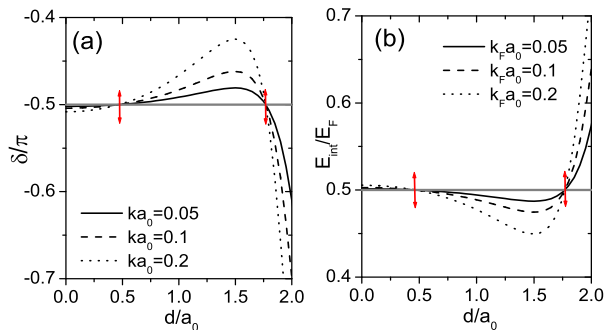


FIG. 5: Universality at SIR in an impurity system for given $a_0/a_s = 1.2$ ($a_0 = 1/\sqrt{m\omega}$). (a) δ_k in terms of $\tilde{d} = d/a_0$ at given $ka_0 = 0.05, 0.1, 0.2$. The double SIR occur at $\tilde{d} = 0.47, 1.77$ (as shown by red arrows), where $\delta_k = -\pi/2$ (gray line) for any k . (b) E_{int}/E_F as a function of \tilde{d} for different fermi momentum $k_F a_0 = 0.05, 0.1, 0.2$. E_{int} shows universal value as $E_F/2$ (gray line) at SIR.

Above impurity problem explicitly shows that *the universal behavior of a many-body system is a direct consequence of the divergent two-body coupling strength and the resulted uniform phase shift in k -space*. This conclusion should generally apply to a wide range of cases, e.g., arbitrary numbers and mass ratios of two-component fermions. In our system, we conclude that within $a_0/a_s \in (0.791, 1.46]$, by increasing \tilde{d} the metastable many-body

scattering state would go across two consecutive universal regimes. At small \tilde{d} it is a crossover from the Fermionic super-Tonks-Girardeau(TG)[17] to Fermionic TG regime, and at large \tilde{d} a reverse process.

VI. EXPERIMENTAL REALIZATION AND FINAL REMARKS

The probing of SIR and its physical consequences can be realized by taking advantage of sophisticated optical techniques to manipulate cold atoms. For two spin-species of the same isotope ($m_A = m_B$), separated harmonic traps can be generated in the setup of spin-dependent optical lattices[18, 19]. The separation d can be tuned by adjusting the polarization angles of two linearly polarized and counterpropagating laser beams (with wavelength λ), which create the lattices. In Ref.[18], the maximum separation between the nearest two species is $d_{max} = 3\lambda/16 \sim 150nm$, comparing to the typical confinement length $a_0 \sim 50nm$. The ratio, $d/a_0 = 0 \sim 3$, is of most interest as shown by Fig.2 and Fig.3. For different isotopes $m_A \neq m_B$, the separated traps can be achieved by fine tuning the laser frequency according to different atomic transition lines for different atoms[8, 20]. In such cold atom systems, the position of SIR can be pinned down by the maximum of atom loss rate[7–9]; g_{1D} can be mapped out from the frequencies of collective modes[7]; the binding energy or interaction energy can be deduced from the shift of peak frequency of atomic transition using rf spectroscopy[10].

Before closing, we emphasize that SIR should fall into a new class of resonance different from magnetic Feshbach resonances and confinement induced resonances. The effect brought about by the trap separation is so generic that it should also hold for other trap geometries or interaction types. Our further studies find that the basic features of SIR, i.e., the non-monotonic evolution of CCBS with the separation and thus the resulted exotic properties of effective scattering strength near resonance, still persist in quasi-2D geometry or in the presence of p-wave interaction[21]. Even in the case of $\omega_A \neq \omega_B$ in our quasi-1D system, where the center-of-mass and relative motions can not be separated, each CCBS emerging from different center-of-mass channels will evolve non-monotonically with \tilde{d} . It is conceivable that for given a_s/a_0 several CCBS could go across the zero threshold energy. This will bring extra interesting resonance properties, such as arbitrarily finite resonance number and novel structure of g_{1D} near resonance. In contrast, for Feshbach resonance or confinement induced resonances, each CCBS monotonically evolves with the magnetic field or confinement length, resulting in infinite number of resonances and the similar structure of effective scattering strength near each resonance[4, 5, 8]. The SIR found at the two-body level also has strong indication for intriguing many-body phenomena, which await full exploration in the future.

We thank Hui Zhai for helpful discussions and comments on the manuscript. Authors XC and ZY thank the Aspen Center for Physics for its hospitality during the cold atom workshop. This work is supported in part by Tsinghua University Initiative Scientific Research Program, NSFC under Grant No. 11104158, NSF Grants DMR-0907366, and by DARPA under the Army Research

Office Grant Nos. W911NF0710464, W911NF0710576.

Appendix A: Derivation of Eq.4

We expand the Green function (Eq.(3) in the text) as

$$G(r, 0) = \phi_{0,0}(x, y)\phi_{0,0}^*(0, 0)e^{ik|z|} \frac{\mu}{ik} - \int_0^\infty dt \sqrt{\frac{\mu}{2\pi t}} e^{-\frac{\mu z^2}{2t} + \frac{k^2 t}{2\mu}} \left(\sum_{n_1=0}^\infty e^{-n_1\omega t} \phi_{n_1}(x)\phi_{n_1}^*(0) \right) \left(\sum_{n_2=0}^\infty e^{-n_2\omega t} \phi_{n_2}(y)\phi_{n_2}^*(0) \right) - \phi_{0,0}(x, y)\phi_{0,0}^*(0, 0), \quad (\text{A1})$$

where we have used imaginary-time integration for the low-energy scattering ($E = \omega + \frac{k^2}{2\mu} < 2\omega$); μ is the reduced mass of two atoms A and B; $\phi_n(x) = \psi_n(x-d)$,

$\phi_n(y) = \psi_n(y)$, and $\psi_n(x) = \frac{1}{\sqrt{N}} H_n(\frac{x}{a_0}) \exp(-\frac{x^2}{2a_0^2})$ is the eigen-state for 1D harmonic oscillator centered at $x=0$ and with characteristic length a_0 .

Further by utilizing the single-particle imaginary-time propagator ($a_0 = 1/\sqrt{\mu\omega}$)

$$\sum_{n=0}^\infty e^{-n\omega t} \psi_n(x)\psi_n^*(x') = \frac{1}{\sqrt{\pi}a_0} \frac{1}{\sqrt{1-e^{-2\omega t}}} e^{-\frac{x^2+x'^2}{2a_0^2} \coth(\omega t) + \frac{xx'}{a_0^2 \sinh(\omega t)}}, \quad (\text{A2})$$

the second term in Eq.A1 is reduced to

$$-\frac{1}{\pi a_0^2} \sqrt{\frac{\mu}{2\pi w}} \int_0^\infty \frac{d\tau}{\sqrt{\tau}} e^{-\frac{k^2 a_0^2 \tau}{2} - \frac{z^2}{2a_0^2 \tau}} \left(\frac{e^{-\frac{(x-d)^2 + (-d)^2}{2a_0^2} \coth \tau + \frac{(x-d)(-d)}{a_0^2 \sinh \tau} - \frac{y^2}{2a_0^2} \coth \tau}}{1 - e^{-2\tau}} - e^{-\frac{(x-d)^2}{2a_0^2} - \frac{d^2}{2a_0^2} - \frac{y^2}{2a_0^2}} \right), \quad (\text{A3})$$

which implicitly includes a divergence as $-\frac{\mu}{2\pi r}$ at small $r = \sqrt{x^2 + y^2 + z^2}$ due to the integration at $\tau \rightarrow 0$. Using the exact relation

$$\int_0^\infty \frac{d\tau}{\tau^{\frac{3}{2}}} e^{-\frac{z^2}{2a_0^2 \tau}} = \sqrt{2\pi} \frac{a_0}{r} \quad (\text{A4})$$

we extract the divergent term from the Green function and rewrite it as

$$G(r, 0) = \phi_{0,0}(x, y)\phi_{0,0}^*(0, 0)e^{ik|z|} \frac{\mu}{ik} - \frac{1}{\pi a_0^2} \frac{\mu a_0}{\sqrt{2\pi}} \int_0^\infty \frac{d\tau}{\sqrt{\tau}} e^{-\frac{k^2 a_0^2 \tau}{2} - \frac{z^2}{2a_0^2 \tau}} \left(e^{-\frac{(x-d)^2 + (-d)^2}{2a_0^2} \coth \tau + \frac{(x-d)(-d)}{a_0^2 \sinh \tau} - \frac{y^2}{2a_0^2} \coth \tau} \frac{1}{1 - e^{-2\tau}} - \frac{e^{-\frac{x^2 + y^2}{2a_0^2} - \frac{k^2 a_0^2 \tau}{2}}}{2\tau} - e^{-\frac{(x-d)^2}{2a_0^2} - \frac{d^2}{2a_0^2} - \frac{y^2}{2a_0^2}} \right) - \frac{\mu}{2\pi r}. \quad (\text{A5})$$

Now it is straightforward to obtain $C(ka_0, \vec{d}) = \frac{\partial}{\partial r}(rG(r, 0))|_{r \rightarrow 0}$ as Eq.(4) and further $A(ka_0, \vec{d})$ as

Eq.(5) in the text.

Appendix B: Property of $A(ka_0, \tilde{d})$

To see the energy-dependence of $A(ka_0, \tilde{d})$, we expand it in terms of small $ka_0 \ll 1$ as $A(ka_0, \tilde{d}) = A(0, \tilde{d}) + \lambda_d (ka_0)^2 + o(k^4 a_0^4)$, with

$$\begin{aligned} \lambda_d &= \int_0^\infty d\tau \frac{\sqrt{\tau}}{2} \left(\frac{e^{-\tilde{d}^2 \tanh \frac{\tau}{2}}}{1 - e^{-2\tau}} - e^{-\tilde{d}^2} \right) \\ &= \begin{cases} 0.409, & d = 0 \\ \frac{\sqrt{2\pi}}{4\tilde{d}}, & \tilde{d} \rightarrow \infty \end{cases} \end{aligned} \quad (\text{B1})$$

Note that due to $\partial\lambda_d/\partial\tilde{d} > 0$ at $\tilde{d} \ll 1$, λ_d increases with \tilde{d} at small \tilde{d} . However, λ_d decrease as $1/\tilde{d}$ at large \tilde{d} . Therefore in the intermediate \tilde{d} , λ_d should reach a maximum determined by $\partial\lambda_d/\partial\tilde{d} = 0$, i.e.,

$$\int_0^\infty d\tau \frac{\sqrt{\tau}}{2} \left(\frac{e^{-\tilde{d}^2 \tanh \frac{\tau}{2}} \tanh \frac{\tau}{2}}{1 - e^{-2\tau}} - e^{-\tilde{d}^2} \right) = 0, \quad (\text{B2})$$

and this gives $\tilde{d} = 1.023$ and $(\lambda_d)_{max} = 0.666$.

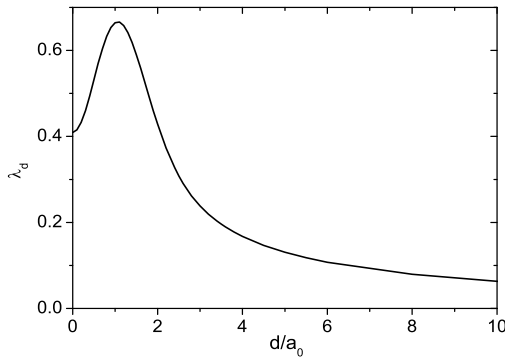


FIG. 6: λ_d (Eq.B1) as functions of the separation \tilde{d} .

The small λ_d obtained for all \tilde{d} justify us to only consider the k -independent part of $A(ka_0, \tilde{d})$ in the scatter-

ing problem,

$$A(0, \tilde{d}) = \int_0^\infty \frac{d\tau}{\sqrt{\tau}} \left(\frac{e^{-\tilde{d}^2 \tanh \frac{\tau}{2}}}{1 - e^{-2\tau}} - \frac{1}{2\tau} - e^{-\tilde{d}^2} \right). \quad (\text{B3})$$

Next we analyze it in two limits.

(1) when $\tilde{d} \rightarrow 0$, $A(0, \tilde{d}) = a + b\tilde{d}^2 + o(\tilde{d}^4)$, with

$$\begin{aligned} a &= \int_0^\infty \frac{d\tau}{\sqrt{\tau}} \left(\frac{1}{1 - e^{-2\tau}} - \frac{1}{2\tau} - 1 \right) \simeq -1.83, \\ b &= \int_0^\infty \frac{d\tau}{\sqrt{\tau}} \left(1 - \frac{\tanh \frac{\tau}{2}}{1 - e^{-2\tau}} \right) \simeq 1.75. \end{aligned} \quad (\text{B4})$$

This gives the resonance value of $[a_0/a_s]_{res} = 1.46 - 1.39\tilde{d}^2$ at small \tilde{d} .

(2) when $\tilde{d} \rightarrow \infty$, Eq.B3 is mostly contributed by small τ . In this limit, Eq.B3 is equivalent to

$$\begin{aligned} A(0, \tilde{d}) &\approx \int_0^\infty \frac{d\tau}{\sqrt{\tau}} \left(\frac{e^{-\tilde{d}^2 \tau/2}}{2\tau(1 - \tau)} - \frac{1}{2\tau} \right) \\ &\approx \int_0^\infty \left[\frac{e^{-\tilde{d}^2 \tau/2} - 1}{2\tau^{3/2}} + \frac{e^{-\tilde{d}^2 \tau/2}}{2\tau^{1/2}} \right] \\ &= \sqrt{\frac{\pi}{2}} (-\tilde{d} + 1/\tilde{d}), \end{aligned} \quad (\text{B5})$$

which gives $[a_0/a_s]_{res} = \tilde{d} - 1/\tilde{d}$ at large \tilde{d} .

Eq.B4 and Eq.B5 show that $A(0, \tilde{d})$ increases with \tilde{d} at small \tilde{d} while decreases at large \tilde{d} . The turning point is given by $\frac{\partial A(0, \tilde{d})}{\partial \tilde{d}} = 0$, i.e.,

$$\int_0^\infty \frac{d\tau}{\sqrt{\tau}} \left(\frac{e^{-\tilde{d}^2 \tanh \frac{\tau}{2}} \tanh \frac{\tau}{2}}{1 - e^{-2\tau}} - e^{-\tilde{d}^2} \right) = 0, \quad (\text{B6})$$

and this gives $\tilde{d} = 1.123$, corresponding to the resonance value of $[a_0/a_s]_{res} = 0.791$ (see also Fig.2(a)).

-
- [1] M. Olshanii, Phys. Rev. Lett. **81**, 938 (1998).
 - [2] T. Bergeman, M. G. Moore and M. Olshanii, Phys. Rev. Lett. **91**, 163201 (2003).
 - [3] D. S. Petrov, M. Holzmann and G. V. Shlyapnikov, Phys. Rev. Lett. **84**, 2551 (2000); D. S. Petrov and G. V. Shlyapnikov, Phys. Rev. A. **64**, 012706 (2001).
 - [4] V. Peano, M. Thorwart, C. Mora and R. Egger, New J. Phys. **7**, 192 (2005).
 - [5] Y. Nishida and S. Tan, Phys. Rev. Lett. **101**, 170401 (2008).
 - [6] H. Moritz, T. Stöferle, K. Günter, M. Köhl and T. Esslinger Phys. Rev. Lett. **94**, 210401 (2005).
 - [7] E. Haller, M. Gustavsson, M. J. Mark, J. G. Danzl, R. Hart, G. Pupillo and H.-C. Nägerl, Science **325**, 1224(2009).
 - [8] G. Lamporesi, J. Catani, G. Barontini, Y. Nishida, M. Inguscio and F. Minardi, Phys. Rev. Lett. **104**, 153202 (2010).
 - [9] E. Haller, M. J. Mark, R. Hart, J. G. Danzl, L. Reichsöllner, V. Melezhik, P. Schmelcher and H.C. Nägerl, Phys. Rev. Lett. **104**, 153203 (2010).
 - [10] B. Fröhlich, M. Feld, E. Vogt, M. Koschorreck, W. Zwerger, M. Köhl, Phys. Rev. Lett. **106**, 105301 (2011).
 - [11] X. Cui, Few Body Systems, doi: 10.1007/s00601-011-0298-6.
 - [12] C. Chin, R. Grimm, P. Julienne and E. Tiesinga, Rev. Mod. Phys. **82**, 1225 (2010).
 - [13] T.-L. Ho and X. Cui, cond-mat/11054627.
 - [14] S. Giraud and R. Combescot, Phys. Rev. A **79**, 043615 (2009).

- [15] X. Cui and H. Zhai, Phys. Rev. A **81**, 041602 (2010); P. Massignan and G. M. Bruun, Eur. Phys. J. D **65**, 83 (2011); R. Schmidt and T. Enss, Phys. Rev. A **83**, 063620 (2011).
- [16] C. Kohstall, M. Zaccanti, M. Jag, A. Trenkwalder, P. Massignan, G. M. Bruun, F. Schreck, R. Grimm, arXiv: 1112.0020.
- [17] L. Guan and S. Chen, Phys. Rev. Lett. **105**, 175301 (2010).
- [18] O. Mandel, M. Greiner, A. Widera, T. Rom, T. W. Hänsch, and I. Bloch, Phys. Rev. Lett. **91**, 010407 (2003).
- [19] D. McKay and B. DeMarco, New J. Phys. **12**, 055013 (2010).
- [20] N. Spethmann, F. Kindermann, S. John, C. Weber, D. Meschede and A. Widera, cond-mat/1109.1639.
- [21] W. Fu and X. Cui (unpublished).